ELSEVIER

Materials Science and Engineering A346 (2003) 254–265

MATERIALS SCIENCE & ENGINEERING A

www.elsevier.com/locate/msea

Investigations on the fracture toughness of austempered ductile iron alloyed with chromium

P. Prasad Rao [a], Susil K. Putatunda [b,*]

[a] Department of Metallurgical and Materials Engineering, Karnataka Regional Engineering College, Surathkal, Karnataka 574 157, India
[b] Department of Chemical Engineering and Materials Science, Wayne State University, 5050 Anthony Wayne Drive, Detroit, MI 48202, USA

Received 1 May 2002; received in revised form 15 July 2002

Abstract

An investigation was carried out to examine the influence of chromium content on the plane strain fracture toughness of austempered ductile iron (ADI). ADIs containing 0, 0.3 and 0.5 wt.% chromium were austempered over a range of temperatures to produce different microstructures. The microstructures were characterized by optical microscopy and X-ray diffraction. Plane strain fracture toughness of all these materials was determined and correlated with microstructure and chromium content. The chromium content was found to influence the fracture toughness through its influence on the processing window. Since the chromium addition shifts the processing window to shorter durations, the higher chromium alloys at higher austempering temperatures tend to fall outside of the processing window, resulting in less than optimum microstructure and inferior fracture toughness. A small chromium addition of 0.3 wt.% was found to be beneficial for the fracture toughness of ADI.

Keywords: Austempered ductile iron; Fracture toughness; Austenite; Ferrite; Alloyed ductile iron; Chromium

1. Introduction

Austempered ductile iron (ADI) is considered to be an important engineering material because of its attractive properties such as good ductility at high strengths, good wear resistance and fatigue strength [1–4]. ADIs are reported to have fracture toughness comparable to those of heat treated medium and low alloy steels [5–12]. The attractive properties of ADI are related to their unique microstructure that consists of ferrite and austenite rather than ferrite and carbide as in steels [1–3]. Because of this, the product of austempering reaction in ductile iron is called as ausferrite rather than bainite. This terminology will be used in the present paper. Large amount of silicon present in ductile iron suppresses the precipitation of carbide during austempering reaction, and retains substantial amount of stable high carbon austenite. Small amounts of alloying elements such as copper, nickel and molybdenum are generally added to ductile iron so that it has sufficient hardenability to be quenched to the austempering temperature without forming pearlite. An important alloying element in low alloy steels that imparts good hardenability is chromium. But because of its deleterious effect on the nodularity of graphite, it is generally not used in ductile irons. When added in amounts less than 1 wt.%, it is not expected to affect the nodularity much.

Production of ADI involves heating the ductile cast iron in the austenitic temperature range between 815 and 927 °C (1500–1700 °F) where the structure becomes fully austenitic (γ). Following this the material is quenched in the austempering temperature range between 260 (500 °F) and 400 °C (750 °F) and held there for 2–4 h. During the austempering process ADI undergoes two stage transformation process. In the first stage, the austenite (γ) decomposes into ferrite and high carbon austenite (γ_{HC}):

$$\gamma \rightarrow \alpha + \gamma_{HC} \quad (1)$$

If the casting is held at the austempering temperature for too long, then a second reaction takes place where the high carbon austenite (γ_{HC}) further decomposes into

* Corresponding author. Tel.: +1-313-577-3808; fax: +1-313-577-3810
E-mail address: sputa@chem1.eng.wayne.edu (S.K. Putatunda).

0921-5093/02/$ - see front matter
PII: S0921-5093(02)00541-5

ferrite and carbide.

$$\gamma_{HC} \rightarrow \alpha + \varepsilon \text{ carbide} \quad (2)$$

The product of this second reaction is undesirable because it embrittles the material and degrades the mechanical properties. Therefore, this reaction is usually avoided during the production of ADI. This time period between the completion of the first reaction and the onset of the second reaction is known as 'process window'. It has been reported that the chromium addition reduces the processing window [13]. The influence may vary considerably with austempering temperature. At low temperatures its influence may be insignificant because the optimum processing duration (OPD) or the process window is rather wide. However, at higher temperatures chromium may have a significant influence on the OPD. Since the austempering temperature and time are known to have a profound effect on fracture toughness of ADI through their influence on microstructure, the chromium addition can be expected to considerably alter the fracture behavior of ADI. Currently, no information is available in literature on the influence of small additions of chromium on the fracture toughness of ADI. The objective of the present investigation was to examine the influence of chromium on microstructure and fracture toughness of ADI.

2. Experimental procedure

Three ductile irons of compositions shown in Table 1 were used in the present investigation. They had similar compositions except for chromium content. While ADI 1 was free of any chromium, ADI 2 and 3 contained 0.3 and 0.5 wt.% chromium, respectively. Compact tension samples were prepared from the cast blocks of these ions as per ASTM standard E-399 [14] and were subjected to austempering heat treatment that consisted of austenitizing at 871 °C (1600 °F) for 2 h and subsequent austempering at four different temperatures for 2 h each. The austempering temperatures selected were 260 (500 °F), 302 (575 °F), 358 (675 °F) and 385 °C (725 °F). The temperatures were so selected that the first two were expected to result in lower ausferitic microstructure, while the last two upper ausferitic microstructure. The as-cast microstructure was predominantly pearlitic in nature.

Table 1
Chemical composition of the three irons in weight percent

Element	ADI 1	ADI 2	ADI 3
C	3.50	3.54	3.50
Si	2.65	2.81	2.47
Mn	0.40	0.43	0.38
S	0.01	0.009	0.01
P	0.021	0.031	0.021
Mg	0.035	0.05	0.035
Cu	0.55	0.56	0.35
Ni	1.60	1.52	1.57
Mo	0.30	0.30	0.30
Cr	Nil	0.30	0.50

The microstructures of heat treated samples were studied by optical microscopy after etching with 2% nital. Volume fraction of retained austenite and its carbon content were estimated by X-ray diffraction technique using a Rigaku rotating head diffractometer with crystal monochromated copper K_α radiation following a technique of Rundman and Klug [15]. Hardness was measured on all the heat-treated samples using Rockwell C scale. Plane strain fracture toughness testing was carried out as per ASTM E-399 [14] on an MTS 810 servohydraulic machine. Fractographic examinations were carried out on stable crack growth regions of the fracture surfaces of the samples on a Hitachi scanning electron microscope to identify the fracture mode. Complete details of the experimental techniques has been presented in the previous publications [11,12].

3. Results and discussion

3.1. Influence of microstructure

The optical microscopic examination revealed that the samples austempered at 260 (500 °F) and 302 °C (575 °F) had lower ausferitic microstructure consisting of very fine needles of ferrite. The samples austempered at the higher temperatures had typical broad ferrite needles of the upper ausferitic microstructure. Fig. 1 shows typical microstructures of ADI 3 at the four austempering temperatures. A gradual change in the microstructure can be observed with rising temperature. Very similar microstructures were observed in ADI 1 and 2 also.

The influence of austempering temperatures on the volume fraction of the retained austenite and its carbon content are reported in Figs. 2 and 3, respectively for the three irons. It can be seen that the retained austenite content generally rises with rising austempering temperature. It increases from a low value of around 20 vol.% at the lowest temperature (260 °C) to a high value of around 40 vol.% at the highest temperature of 385 °C (725 °F). On the other hand, the variation in the carbon content of the retained austenite shows a different behavior. It increases when the austempering temperature is raised from 260 (500 °F) to 302 °C (575 °F) and then drops with further rise in temperature. The variation in the volume fraction of the retained austenite and its carbon content with austempering temperature is similar to that reported by other investigators and can

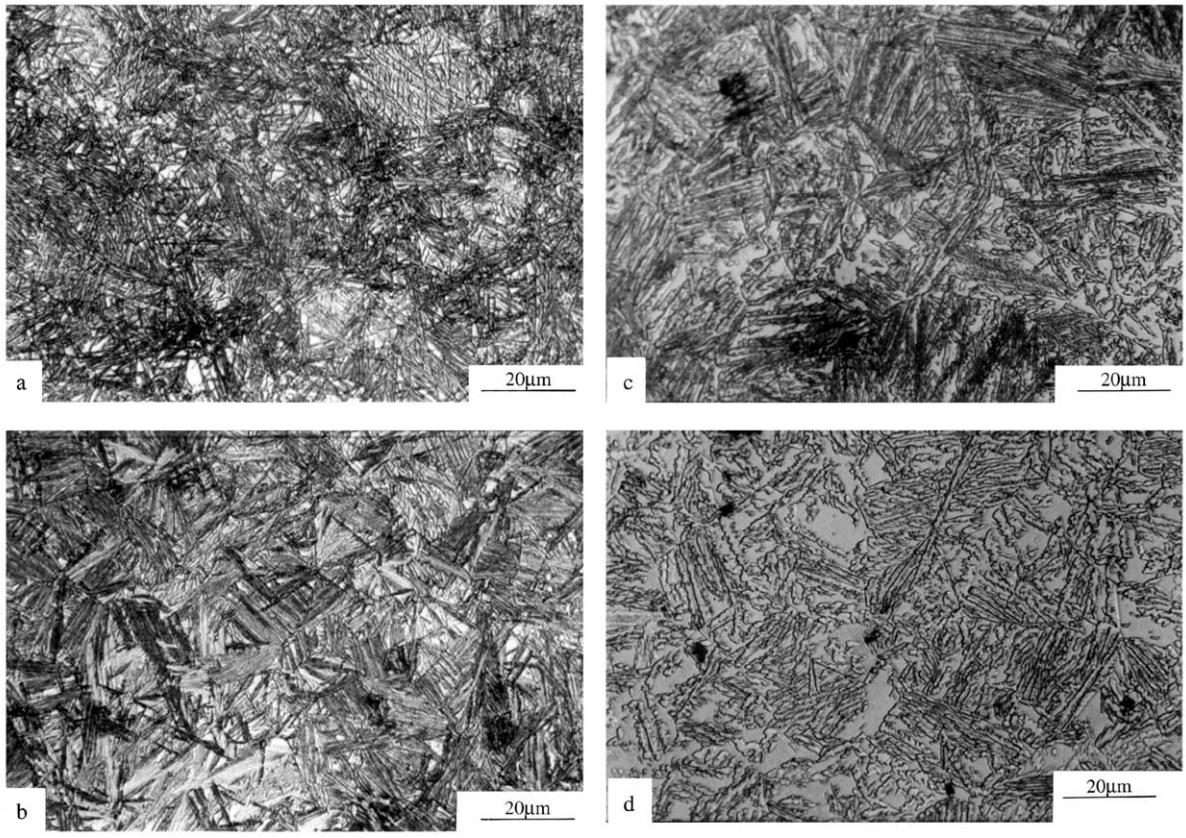

Fig. 1. (a) Microstructure of ADI 3 after austempering for 2 h at 260 °C (500 °F). (b) Microstructure of ADI 3 after austempering for 2 h at 302 °C (575 °F). (c) Microstructure of ADI 3 after austempering for 2 h at 357 °C (674 °F). (d) Microstructure of ADI 3 after austempering for 2 h at 385 °C (725 °F).

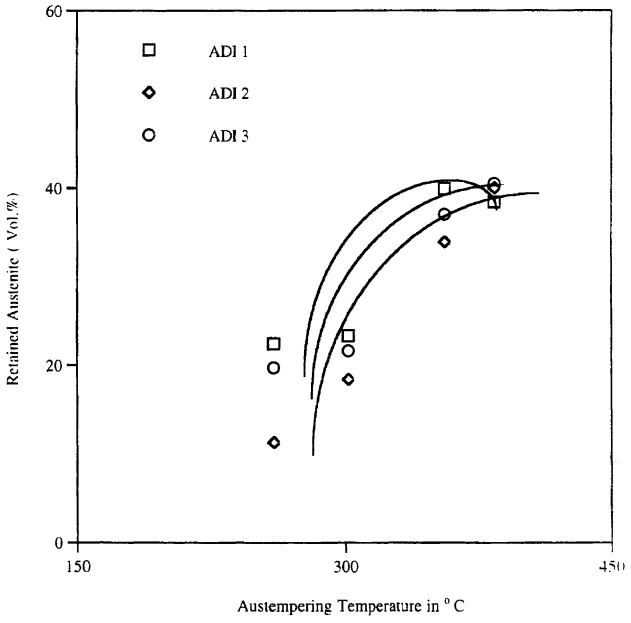

Fig. 2. Influence of austempering temperature on volume fraction of austenite.

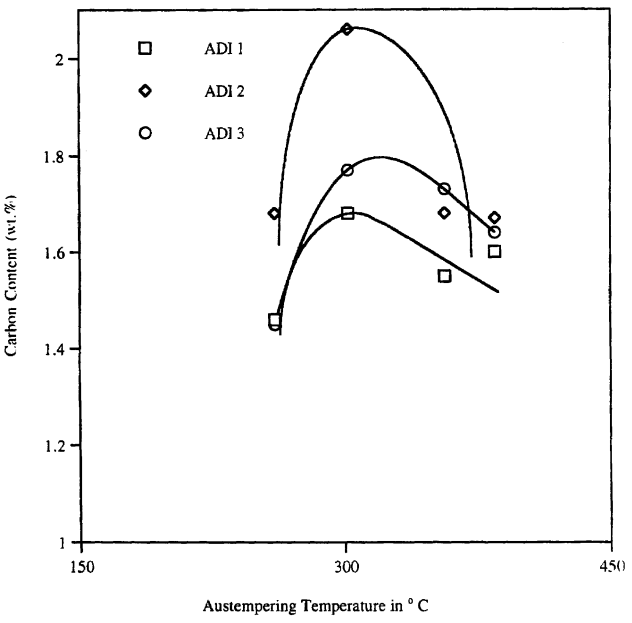

Fig. 3. Influence of austempering temperature on carbon content (C_γ) of austenite.

be explained on the basis of kinetics of ferrite formation and diffusion of carbon in austenite [16–18].

The initial carbon content (C_O) of the austenite at a given austenitizing temperature is given by the following expression [19]:

$$C_O = (T_\gamma/420) - 0.17(\mathrm{Si}) - 0.95, \quad (3)$$

where T_γ is the austenitizing temperature in °C and Si is the silicon content in wt.%. In the present investigation T_γ is 871 °C and Si content ranges from 2.47 to 2.81 wt.%. Substituting these values in the above equation, C_O is found to be in the range of 0.67 for ADI 1 to 0.70 for ADI 3. This is the carbon content of the austenite at the austenitizing temperature. How much of this carbon finds its way into the retained austenite depends on the kinetic factors and is given by the parameter $X_\gamma C_\gamma$, which is called as the matrix carbon (here X_γ is the volume fraction of retained austenite and C_γ is its carbon content). Table 2 reports the initial carbon content C_O and the matrix carbon content ($X_\gamma C_\gamma$) for all three alloys. Table 2 shows that the matrix carbon is nearly equal to C_O at the higher austempering temperatures, but much less than C_O at the lower temperatures. The trend is same in all the three irons. This means at higher austempering temperatures due to faster diffusion of carbon most of the carbon (C_O) finds its way into the austenite where as at lower temperatures it does not.

The plane strain fracture toughness of all the three irons was determined under all the heat treatment conditions. Five identical samples were tested in each case, and the results reported are an average of these. Standard deviation in each case was less than 1.00 MPa$\sqrt{m}$. Results are reported in Table 2. Fig. 4 is a plot of the fracture toughness against the austempering temperature at the three chromium levels. The fracture toughness initially increased with increasing austempering temperature, reached a maximum at an intermediate temperature and decreased with further rise in temperature. This behavior was observed to be similar at all three chromium levels. ADIs austempered at lower temperatures generally exhibited better fracture toughness than those austempered at higher temperatures. Optimum fracture toughness was obtained when austempering was carried out at 302 °C (575 °F). In fact at all the three chromium levels in the present investigation maximum fracture toughness was observed at 302 °C (575 °F).

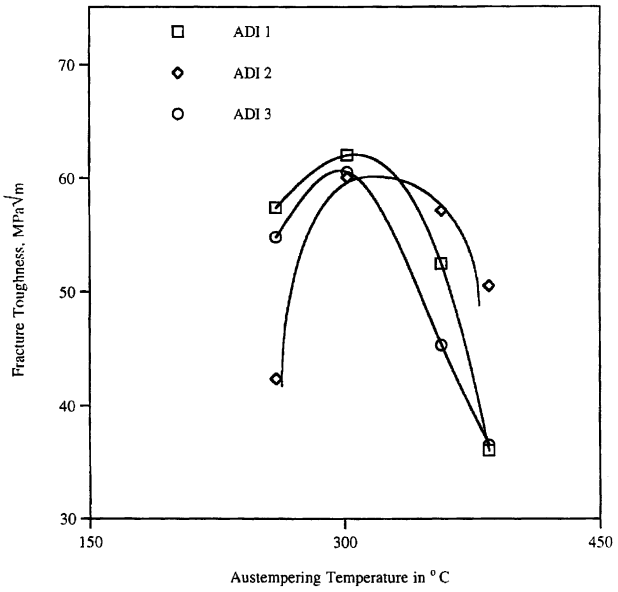

Fig. 4. Influence of austempering temperature on fracture toughness.

The fracture surfaces of the fracture toughness samples were studied under the scanning electron microscope to elicit information on the fracture mode. Fig. 5 shows the fractographs of ADI 3 and 1 under different austempering conditions. While the samples austempered at 260 (500 °F) and 302 °C (575 °F) showed predominantly dimpled ductile fracture, the one austempered at 385 °C (725 °F) showed fully

Table 2
Carbon content, hardness and fracture toughness values under different heat treatment conditions

Iron	Austempering temperature (°C)	Retained austenite (vol.%)	Carbon content of austenite (C_γ) (wt.%)	$X_\gamma C_\gamma$	Hardness HRC	K_{IC} (MPa$\sqrt{m}$)
ADI 1	260	22.4	1.46	0.33	47	57.4
	302	23.3	1.68	0.39	44	62.01
	357	39.9	1.55	0.62	33	52.45
	385	38.4	1.60	0.61	31	36.02
ADI 2	260	11.3	1.68	0.19	48	42.36
	302	18.4	2.06	0.38	43.6	60.04
	358	33.9	1.68	0.57	34.8	57.16
	385	40.0	1.67	0.67	31.5	50.51
ADI 3	260	19.7	1.45	0.29	48.1	54.79
	302	21.6	1.77	0.38	43.4	60.54
	358	37.0	1.73	0.64	33.2	45.33
	385	40.5	1.64	0.66	31.1	36.54

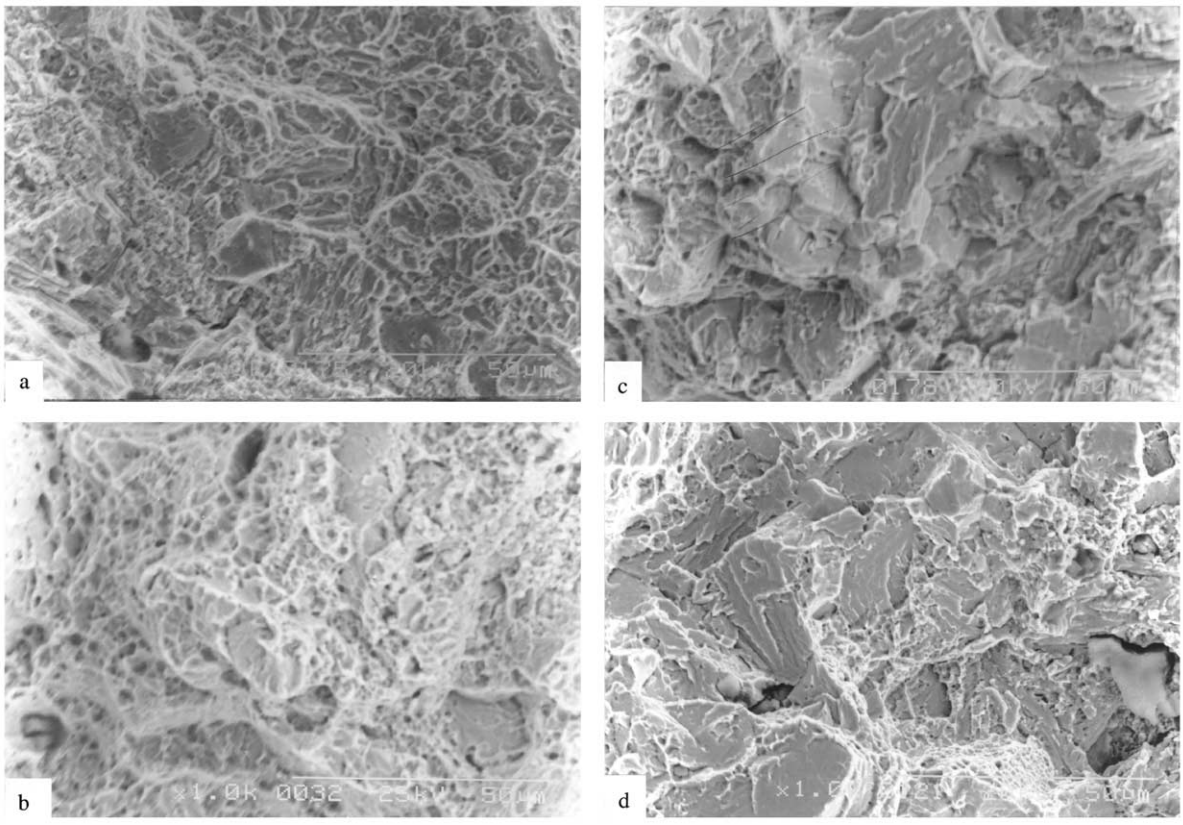

Fig. 5. (a) Fractographs of ADI 1 after austempering at 260 °C (500 °F). (b) Fractographs of ADI 1 after austempering at 302 °C (575 °F). (c) Fractographs of ADI 1 after austempering at 358 °C (675 °F). (d) Fractographs of ADI 1 after austempering at 385 °C (725 °F).

cleavage type of brittle fracture. When austempered at 358 °C (675 °F) a quasi-cleavage fracture was observed. Thus the change in the fracture mode with rising austempering temperature fully corresponds to the change in the fracture toughness values. Fig. 6 shows the fractographs of ADI 2 at the four austempering temperatures. The sample austempered at 260 °C (500 °F) showed mostly intercrystalline type of brittle fracture, while those at 302 (575 °F) and 358 °C (675 °F) showed dimpled fracture. The samples austempered at 385 °C (725 °F) showed high-energy tear fracture. As in ADI 1, here too, the fracture modes fully reflect the fracture toughness values at the different austempering temperatures. Fig. 7 shows the fractographs of ADI 3. Only the sample austempered at 302 °C (575 °F) showed ductile fracture. The one austempered at 260 °C (500 °F) showed predominantly cleavage fracture. So also the sample austempered at 358 °C (675 °F). But in this a tendency towards intercrystalline fracture could be noticed. At 385 °C (725 °F), the fracture was essentially intercrystalline brittle type.

The results of the microstructure and fracture studies can be summarized as follows:

i) When austempered at 302 °C (575 °F), all the three irons exhibited dimpled ductile fracture. These had the highest fracture toughness, greater than 60 MPa$\sqrt{m}$. Their microstructures consisted of lower ausferrite with an average austenite content of 20 vol.%. Amongst the four austempering temperatures, the carbon content of the retained austenite was the maximum, in all the three irons, at this temperature.

ii) When austempered at 260 °C (500 °F) the fracture toughness was in the upper fifties. The fracture mode was mixed dimpled and cleavage types. Only ADI 2 at 260 °C (500 °F) showed a different type of fracture. Microstructure was lower ausferrite with very fine ferrite needles. The retained austenite content was very low, and so also the carbon content of retained austenite.

iii) At the higher temperature of 358 °C (675 °F) the fracture toughness was in the lower fifties than at 302 °C. Fracture mode was generally cleavage type with some dimples. Microstructure was upper ausferrite with large retained austenite content and fairly high carbon content.

iv) At the highest temperature of 385 °C (725 °F), the microstructure was the coarsest, and the fracture toughness was the lowest. Even though it had the highest retained austenite content, fracture toughness was still very low.

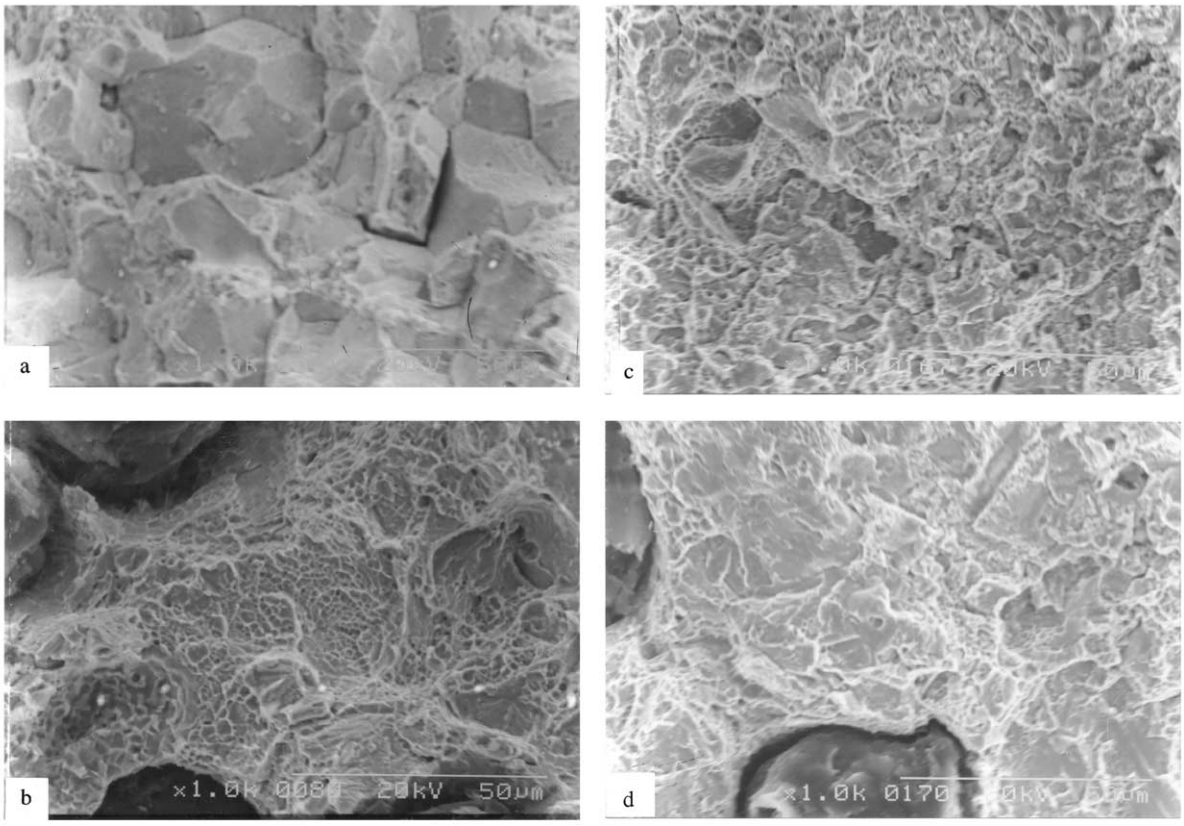

Fig. 6. (a) Fractographs of ADI 2 after austempering at 260 °C (500 °F). (b) Fractographs of ADI 2 after austempering at 302 °C (575 °F). (c) Fractographs of ADI 2 after austempering at 358 °C (675 °F). (d) Fractographs of ADI 2 after austempering at 385 °C (725 °F).

The results of the present investigation agree with the earlier results [11,12] that when the as-cast microstructure is pearlitic in nature, the ADI with the lower ausferrite microstructure has better fracture toughness than that with the upper ausferrite microstructure, and that the optimum fracture toughness is obtained at 302 °C (575 °F) [9–12]. In fact, at all the three chromium levels in the present investigation, the best fracture toughness was observed on austempering at 302 °C (575 °F). All the three irons had pearlitic as-cast structure. The present results also agree with the earlier conclusion that for the optimum fracture toughness, the retained austenite content should be around 25 vol.%, and its carbon content should be as high as possible [12]. The combined effect of these two parameters on the fracture toughness is shown in Fig. 8 as a plot of the fracture toughness against the matrix carbon, $X_\gamma C_\gamma$. This shows a peak at $X_\gamma C_\gamma$ value of 0.45. If the microstructure had retained austenite content of 25 vol.%, this would correspond to a carbon level of 1.8 wt.%.

It has been shown that fracture toughness of ADI depends on microstructural features such as retained austenite content and its carbon content, and morphology of the ausferrite [12,21]. It has been shown that the following relationship between the fracture toughness and the above microstructural features is obeyed [20]:

$$K_{IC}^2 \propto (X_\gamma C_\gamma / d)^{1/2}, \quad (4)$$

where d is the ferrite particle size. The value of 'd' can be determined by the well-known Scherrer equation:

$$d = \frac{0.9\lambda}{B \cos \theta},$$

where λ is the wavelength; θ is the diffraction angle and B is the half width of the diffraction peak. The diffraction peak from {211} planes of ferrite can be used to determine the value of d. The smaller the ferrite particle size, the broader will be the diffraction peak where as the coarser ferrite will give narrower diffraction peaks. Thus, ADI austempered at lower temperature has smaller value of d whereas when ADI is austempered at higher temperature it has larger value of d.

The yield strength of ADI has been related to both austenite content and the ferritic particle size. Harynen et al. [21] and Ali et al. [22] have shown that the yield strength of ADI can be expressed as:

$$\sigma_y = (\sigma_0 + Ad^{-1/2} + BX_\gamma),$$

where d is the ferrite particle size, X_γ is volume fraction of austenite and σ_0, A and B are constants. These authors have also pointed out that A is very large

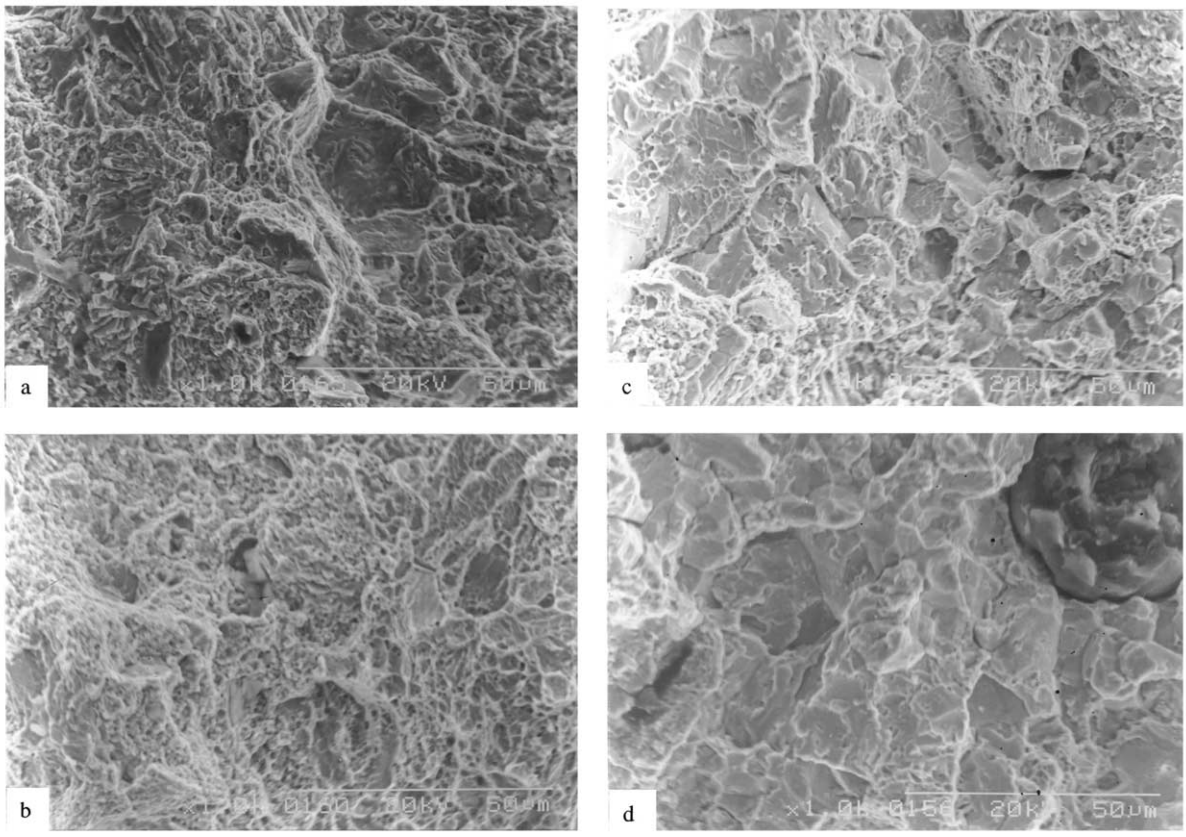

Fig. 7. (a) Fractographs of ADI 3 after austempering at 260 °C (500 °F). (b) Fractographs of ADI 3 after austempering at 302 °C (575 °F). (c) Fractographs of ADI 3 after austempering at 358 °C (675 °F). (d) Fractographs of ADI 3 after austempering at 385 °C (725 °F).

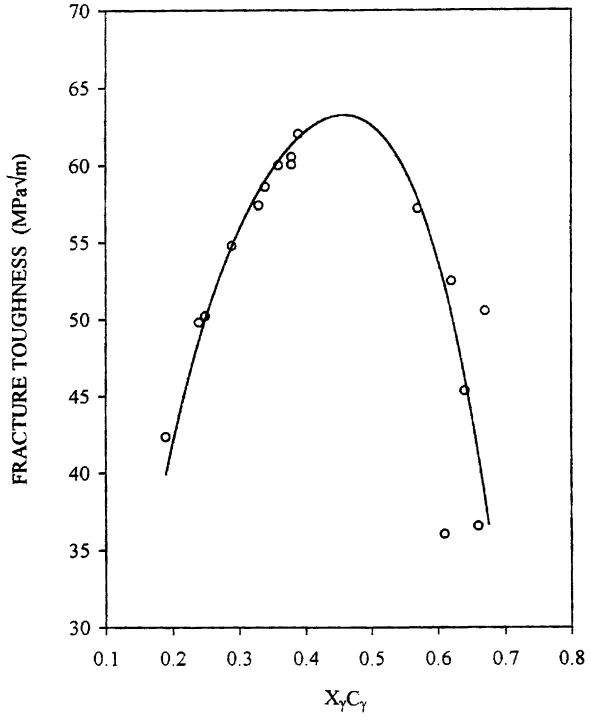

Fig. 8. Influence of matrix carbon $X_\gamma C_\gamma$ on fracture toughness.

compared to B and σ_0. Therefore, the yield strength of ADI is primarily decided by the ferrite particle size i.e.

$$\sigma_y \propto d^{-1/2}.$$

Therefore, from Eq. (4) we can deduce,

$$K_{IC}^2 \propto \sigma_y (X_\gamma C_\gamma)^{1/2}. \quad (5)$$

Generally, materials exhibit a direct relationship between strength and hardness. Therefore, if we replace strength (σ_y) by hardness (H) in the above equation, we get:

$$K_{IC}^2 \propto H (X_\gamma C_\gamma)^{1/2}. \quad (6)$$

The measured values of X_γ, C_γ and H at different austempering temperatures in the three irons are reported in Table 2 along with the fracture toughness values. A plot of K_{IC}^2 against the parameter $H(X_\gamma C_\gamma)^{1/2}$ is shown in Fig. 9. A straight line was drawn through the points by the method of least squares. Regression coefficient was found to be 0.92 showing that the linear relationship of Eq. (6) is obeyed remarkably well by all the three irons.

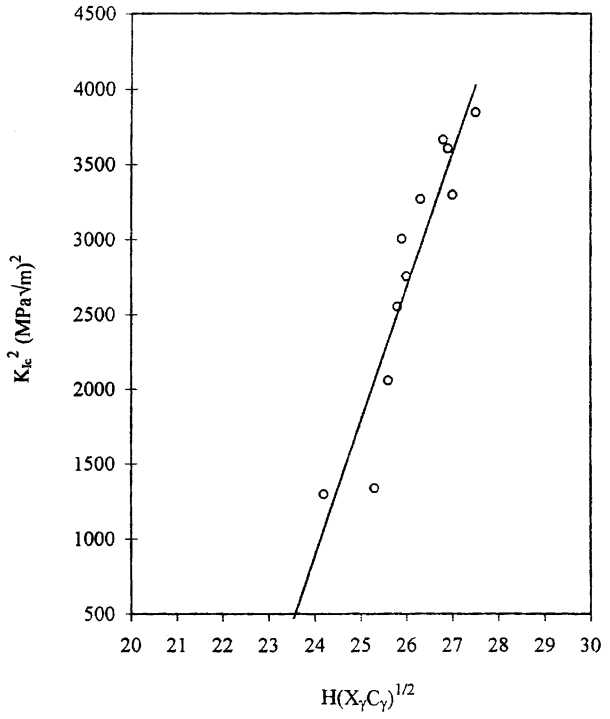

Fig. 9. Plot of K_{IC}^2 against $H(X_\gamma C_\gamma)^{1/2}$.

3.2. Influence of chromium

The relative magnitudes of the fracture toughness at lower and higher austempering temperatures was found to depend on chromium content. This is brought out well in Fig. 10, which shows a plot of fracture toughness against chromium content at the four austempering temperatures. At 302 °C (575 °F) the fracture toughness was practically independent of the chromium content. But at a lower temperature 260 °C (500 °F) it went through a minimum with increasing chromium content, while at higher temperatures it passed through a maximum. Thus the influence of chromium content on fracture toughness is found to be rather complex. This can be related to its influence on microstructure. Microstructure in turn depends on austempering temperature and time. In the present investigation, the austempering time was kept constant at 2 h while the austempering temperature was varied. It should be noted that at any given austempering temperature, there is an optimum austempering time which gives the best results.

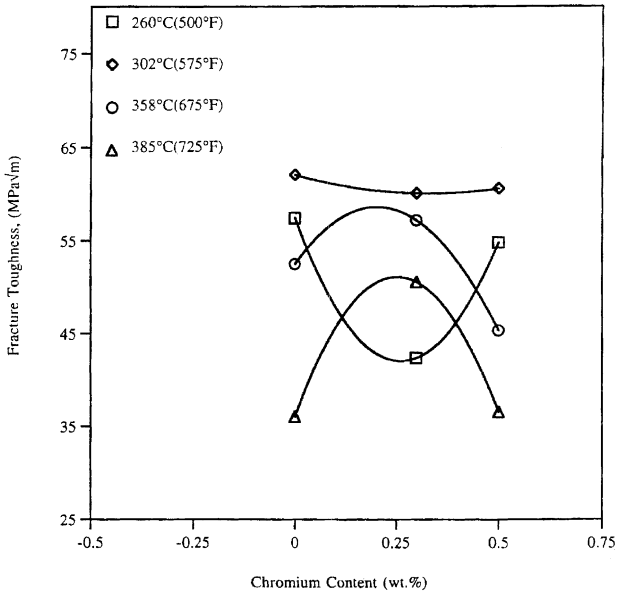

Fig. 10. Influence of chromium content on the fracture toughness of three irons.

As mentioned earlier the austempering reaction in ductile iron consists of the two stages as given below [1,2]:

Stage I $\gamma \rightarrow \alpha + \gamma_{HC}$

Stage II $\gamma_{HC} \rightarrow \alpha + \varepsilon$ carbide

Optimum properties are obtained when ductile iron is austempered such that Stage I is complete and Stage 2 has not yet started. The microstructure then consists of ferrite and stable high carbon austenite. If austempered for too short duration, some untransformed austenite will be present which will transform to martensite. If austempered for too long Stage 2 reaction will set in and carbide precipitation will occur. Both these will embrittle the iron. The OPD or the process window therefore depends on austempering temperature and is shown schematically in Fig. 11. This consists of two curves shown as t_1, and t_2 corresponding, respectively to end of Stage 1 and start of Stage 2 reactions. The time t_1 decreases with the decrease in austempering temperature, since increasing supercooling accelerates the formation of ferrite from austenite. On the other hand t_2 increases with decreasing temperature since slower diffusion rates at lower temperatures retard the carbide precipitation. This interval $(t_2 - t_1)$ is called as processing window or OPD.

The processing window depends on austenitizing temperature and alloy content. Increasing austenitizing temperature and addition of alloying elements such as nickel, copper and molybdenum shifts processing window to longer durations and make heat treatment periods convenient from practical point of view. Thus ADIs generally contain 1.5% nickel, 0.6% copper and 0.3% molybdenum, which is the composition of iron 1 in the present investigation. Irons 2 and 3 contain, in addition, 0.3 and 0.5 wt.%, respectively of chromium. Manganese is known to shift processing window to shorter durations. This is because of its strong tendency to segregate to intercellular regions and draw carbon along with it. It has been reported that chromium also shifts processing window to shorter durations. It has been shown that chromium in large amounts such as 0.4

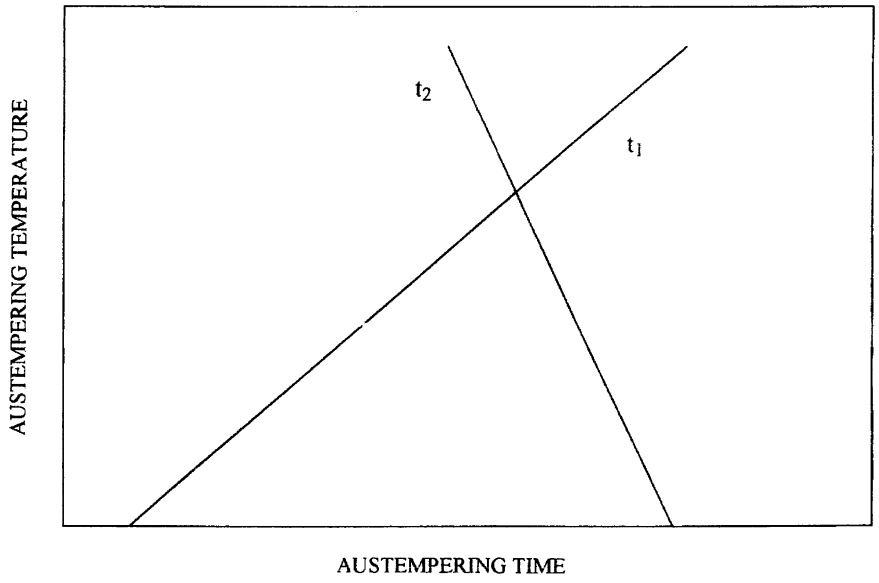

Fig. 11. Schematic representation of dependence of OPD on austempering temperature.

and 0.6 wt.% has very adverse effect on processing window even at a large nickel content of 3.0 wt.%. It was found that OPD dropped from 180–200 min at 0.2 wt.% to 60–120 min at 0.4 wt.% chromium and finally to 15–60 min at 0.6 wt.% chromium when austempered at 350 °C. Thus it is seen that chromium not only decreases t_1, but also decreases the interval (t_2-t_1). The decrease in t_1, can be attributed to the fact that chromium is a strong ferrite stabilizer. It therefore accelerates the Stage 1 reaction. Since chromium also has a strong carbide-forming tendency it decreases t_2 also. The durations mentioned above can be expected to be still lower when nickel content is only 1.5 wt.% as in the present case. However, the lower nickel content may to some extent be compensated by the presence of copper and molybdenum. Fig. 12 shows schematically influence of chromium content on processing window.

The vertical line in this Fig. 12 corresponds to the austempering time of 120 min. *A*, *B*, *C* and *D* correspond to the four austempering temperatures of

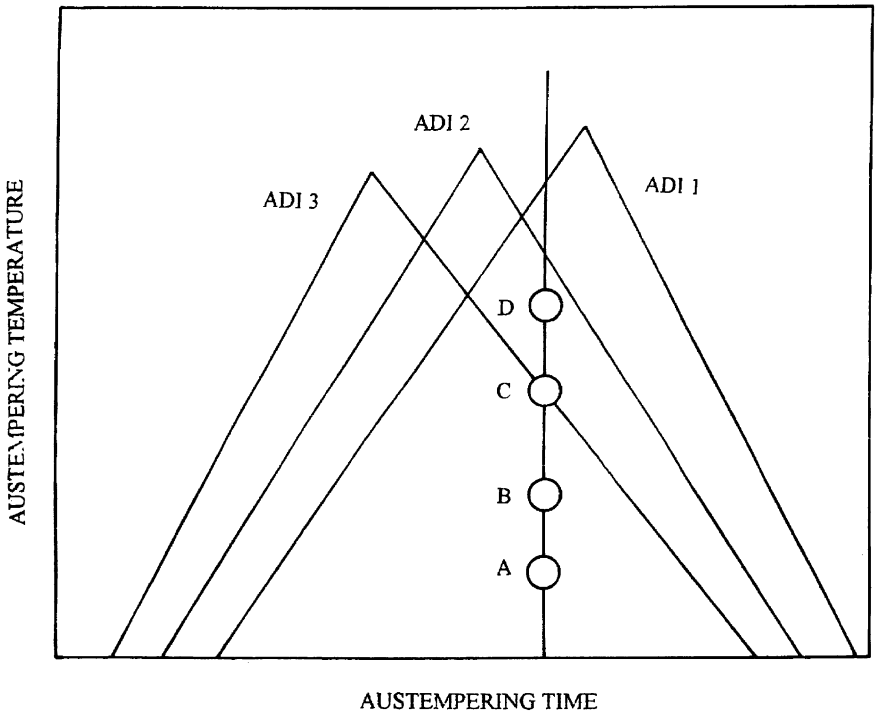

Fig. 12. Schematic plot of processing window at different chromium contents.

260 (500 °F), 302 (575 °F), 358 (675 °F) and 385 °C (725 °F), respectively. With regard to the processing window of iron 1, all the four points are well within the processing window as to be expected from the results of the previous investigation [12]. These are within the processing window for iron 2 also, even though processing window is shifted to shorter durations. Samples austempered at 302 °C (575 °F) higher temperatures showed better fracture toughness. This is most likely due to the higher carbon content of the retained austenite in these samples. A strong influence of carbon content of austenite on the fracture toughness of ADI has been reported by Putatunda et al. [11,12]. Microstructures of ADI 2 samples were relatively finer than ADI 1 and 3. Because of these, it is found that the fracture toughness values after austempering at different temperatures are within a narrower range in ADI 2 as compared to 1. Finally, the processing window of ADI 3 is such that D, and possibly C will lie outside as shown in the figure. This will promote extensive carbide precipitation during austempering as Stage 2 reaction will have set in. Since this takes place primarily in the intercellular regions, intergranular fracture is to be expected. Samples austempered at 385 °C (725 °F) showed extensive intergranular fracture for ADI 3 while those austempered at 358 °C (675 °F) showed initial stages of intergranular fracture suggesting that location of processing window for ADI 3 as shown in the Fig. 12 is indeed correct. No evidence of carbide precipitation could be noticed in the XRD profiles. This is because of the low intensity of the carbide peaks and their close proximity to strong peaks of austenite and ferrite [22,23]. It is generally difficult to detect these by X-ray diffraction technique.

The results of the present investigation thus indicate that a small addition of chromium to the extent of 0.3 wt.% has beneficial effect on the fracture behavior of ADI. It considerably narrows the range of fracture toughness values in samples austempered over a wide temperature range. This has very important practical implications. It is generally observed that ADIs austempered at higher temperatures have better tensile toughness and fatigue strength [21,23]. However, as reported in the present investigation and previous studies [9–12], these have generally poor fracture toughness. With proper alloying of ductile iron with chromium, it will be possible to get a good combination of tensile toughness, fatigue strength and fracture toughness in ADI. This aspect needs further investigation.

3.3. Influence of matrix carbon

It is observed from Fig. 8, the matrix carbon $X_\gamma C_\gamma$ has a strong influence on fracture toughness. However, large value of $X_\gamma C_\gamma$ [11,12] by itself is not sufficient to increase the fracture toughness. The other equally important parameter is the morphology of the ferrite. Very fine ferrite together with a large value of $X_\gamma C_\gamma$ is necessary for high fracture toughness. Samples which had matrix carbon greater than 0.5 in Fig. 8 were associated with upper ausferrite microstructure. Therefore, these had lower fracture toughness. The ferrite morphology appears as σ_y in Eq. (4), as $d^{-1/2}$ in Eq. (5) or as H in Eq. (6). Samples with upper ausferritic structure have coarse ferrite, large d, and small σ_y and H. Therefore, even though matrix carbon is large, fracture toughness is low. There is no scope for increasing the fracture toughness of these samples as the matrix carbon ($X_\gamma C_\gamma$) has already reached the maximum (i.e. very close to C_O Table 3). On the other hand, samples with lower ausferritic structure (e.g. samples austempered at 260 (500 °F) and 302 °C (575 °F) have a potential to attain higher fracture toughness, if one can raise their matrix carbon. Low matrix carbon implies that not all the carbon in the original austenite (C_O) has found its way into the retained austenite. This may be present either in solid solution in ferrite or as carbide at the austenite/ferrite interface. If held for sufficiently long time at the austempering temperature, some of this carbon may eventually find its way into the retained austenite. The higher matrix carbon ($X_\gamma C_\gamma$) in such samples should then increase the fracture toughness. In order to examine the validity of this hypothesis, some additional samples from all three irons were austempered at 260 °C (500 °F) for longer duration of 3 and 4 h and values of fracture toughness of these irons austempered for longer durations such as 3 and 4 h and 260 °C (500 °F) were compared with those austempered for 2 h. The result is shown in Table 4. All these samples had similar lower ausferritic microstructures where as matrix carbon ($X_\gamma C_\gamma$) of these samples changed with austempering time. ADI 1 showed a gradual rise in matrix carbon content with increasing time. There was also an appreciable increase in the fracture toughness as there is very little increase in matrix carbon. In ADI 2, there was a large increase in the matrix carbon from 2 to 3 h and only a marginal rise thereafter. Correspondingly, there was a large initial increase in the fracture toughness followed by a marginal rise. ADI 3 showed only a marginal rise in the fracture toughness. It is thus observed that raising the matrix carbon has a beneficial effect on the fracture toughness of ADI. The fracture toughness values of these samples when plotted against the matrix carbon fit well with the curve of Fig. 8.

4. Conclusions

(1) At all the three chromium levels it is found that ADI with lower ausferrite structure has better fracture toughness than that with upper ausferrite. Best fracture toughness was observed in ADI austempered at 302 °C (575 °F).

Table 3
Initial carbon content of austenite (C_O) and the matrix carbon ($X_\gamma C_\gamma$)

Iron	Austempering temperature (°C)	Initial carbon content of austenite (C_O)	Matrix carbon ($X_\gamma C_\gamma$)
ADI 1	260	0.67	0.33
	302		0.39
	358		0.62
	385		0.61
ADI 2	260	0.65	0.19
	302		0.38
	358		0.57
	385		0.65
ADI3	260	0.70	0.29
	302		0.38
	358		0.64
	385		0.66

Table 4
The three irons austempered at 260 °C (500 °F) for different durations

Iron	Austempering time (h)	Matrix carbon ($X_\gamma C_\gamma$)	Fracture toughness (MPa$\sqrt{}$m)
ADI 1	2	0.33	57.4
	3	0.35	58.5
	4	0.36	59.8
ADI 2	2	0.19	42.4
	3	0.24	50.8
	4	0.26	51.6
ADI 3	2	0.29	54.8
	4	0.32	55.2

(2) A plot of fracture toughness against $X_\gamma C_\gamma$ shows a peak which suggests that there is an optimum combination of X_γ and C_γ at which best fracture toughness is obtained, which are 25 vol.% and 1.8 wt.%, respectively.

(3) The results of the present investigation show that K_{IC}^2 is proportional to $\sigma_y(X_\gamma C_\gamma)^{1/2}$. Therefore, fracture toughness can be maximized by maximizing σ_y and the matrix carbon $X_\gamma C_\gamma$.

(4) Chromium content influences the fracture toughness through its influence on the processing window. Since chromium shifts processing window to shorter durations, higher chromium alloys at higher temperatures tend to fall outside of the processing window. This results in less than optimum microstructure and inferior fracture toughness.

(5) A small chromium addition of 0.3 wt.% has beneficial effect on the fracture toughness. It improves the fracture toughness of ADIs with upper ausferrite while retaining the good fracture toughness of ADIs with lower ausferrite.

Acknowledgements

The work was financially supported by Ford Motor Company, Dearborn, Michigan.

References

[1] J.F. Janowak, R.B. Gundlach, AFS Trans. 91 (1983) 377.
[2] J.F. Janowak, R.B. Gundlach, G.T. Eldis, K. Rohrig, I'nt. Cast Metals J. 6 (1981) 28.
[3] M. Johansson, AFS Trans. 85 (1977) 117.
[4] I. Schmidt, A. Schuchert, Zeit. Metalkunde 78 (1987) 871.
[5] K. Zum Ghar, B.L. Wagner, Arch. Eisenhutenwes. 50 (1979) 269.
[6] S.C. Lee, C.C. Lee, AFS Trans. 96 (1988) 827.
[7] J.L. Doong, C.S. Chen, Fatigue Fract. Eng. Mater. Struct. 12 (1989) 155.
[8] J. Aranzabal, I. Gutierrez, J.M. Rodriguez Ibabe, J.J. Urcola, Mater. Sci. Technol. 8 (1992) 263.
[9] I. Bartoziewicz, I. Singh, F.A. Alberts, A.R. Krause, S.K. Putatunda, J. A/fater. D'g. Perform. 4 (1995) 90.
[10] S.K. Putatunda, I. Singh, J. Testing. Eval. 23 (1995) 325.
[11] S. Putatunda, R. Gupta, P.P. Rao, in: M.G. Burke, E.A. Clarke, E.J. Palmiere (Eds.), Understanding Microstructure: Key to Advances in Materials, Proceedings of the 29th ASTM of Int. Metallographic Soc., ASM International, Materials Park, OH, 1996, p. 103.
[12] P.P. Rao, S.K. Putatunda, Metal. Mater. Trans. A 28A (1997) 1457.
[13] A.L. Muralidhara, P.P. Rao, AFS Trans. 96 (1988) 387.
[14] ASTM E-399 Annual Book of ASTM Standards, vol. 03.01, ASTM, Philadelphia, PA, 1992, p. 745.
[15] K.B. Rundman, R.C. Klug, AFS Trans. 90 (1982) 499.

[16] T.N. Rouns, K.B. Rundman, D.M. Moore, AFS Trans. 92 (1984) 815.
[17] N. Darwish, R. Elliott, Mater. Sci. Technol. 9 (1993) 572.
[18] N. Darwish, R. Elliott, Mater. Sci. Technol. 9 (1993) 586.
[19] R.C. Voigt, C.R. Loper, Proc. 1st Int. Conf. on Austempered Ductile Iron, ASM, Metals Park, OH, 1984, p. 83.
[20] P.P. Rao, S.K. Putatunda, Mater. Sci. Technol. 14 (1998) 1257.
[21] P. Shanmugam, P.P. Rao, K.R. Udupa, N. Venkataraman, J. Mater. Sci. 29 (1994) 4933.
[22] P.P. Rao, Indian J. Eng. Mater. Sci. 2 (1995) 24.
[23] L. Barosiewicz, A.R. Krause, F.A. Alberts, I. Singh, S.K. Putatunda, Mater. Charact. 30 (1993) 221.